ACADEMIC PRESS

Available online at www.sciencedirect.com
SCIENCE DIRECT®

Journal of Catalysis 214 (2003) 78–87

JOURNAL OF CATALYSIS

www.elsevier.com/locate/jcat

Influence of oxygen-containing surface groups on the activity and selectivity of carbon nanofiber-supported ruthenium catalysts in the hydrogenation of cinnamaldehyde

Marjolein L. Toebes,[a] Frans F. Prinsloo,[b] Johannes H. Bitter,[a] A. Jos van Dillen,[a] and Krijn P. de Jong [a,*]

[a] *Department of Inorganic Chemistry and Catalysis, Debye Institute, Utrecht University, PO Box 80 083, 3508 TB Utrecht, Netherlands*
[b] *Sasol Technology R&D, PO Box 1, Sasolburg 9570, South Africa*

Received 30 May 2002; revised 12 August 2002; accepted 26 September 2002

Abstract

Carbon-nanofiber-supported ruthenium catalysts were employed to study the influence of oxygen-containing surface groups on catalytic performance in the liquid-phase hydrogenation of cinnamaldehyde. The carbon nanofibers were oxidized to introduce oxygen-containing groups and the metal precursor was applied using homogeneous deposition precipitation. After reduction the catalysts were heat-treated in nitrogen at different temperatures to tune the number of surface oxygen functional groups. TEM and chemisorption studies showed the presence of a narrow and stable particle-size distribution (1–2 nm) even after heat treatment at 973 K. The overall specific activity increased by a factor of 22 after treatment at 973 K, which is related to the decreasing number of oxygen-containing groups. The cinnamyl alcohol selectivity decreases from 48 to 8% due to enhanced rate of hydrocinnamaldehyde production with increasing heat treatment. This unambiguously demonstrates the metal–support interaction, which involves support surface-oxygen functionalities that affect the metal activity and selectivity. The precise nature of this interaction has yet to be elucidated.

Keywords: Carbon nanofibers; CNF; Ruthenium catalyst; Oxygen-containing surface groups; Cinnamaldehyde hydrogenation; Homogeneous deposition precipitation; Metal–support interaction

1. Introduction

Using the hydrogenation of cinnamaldehyde to cinnamyl alcohol as a test reaction we investigated the influence of the concentration of oxygen-containing surface groups on the activity and selectivity of carbon nanofiber (CNF)-supported ruthenium catalysts.

Catalytic hydrogenation of α,β-unsaturated aldehydes to their corresponding alcohols is attractive for both economical and scientific reasons [1–4]. Although hydrogenation of the C=C is thermodynamically more favorable, attempts have been made to enhance the selective hydrogenation of the C=O bond. With ruthenium as the active metal, high selectivities are attained only if titania and carbon, notably graphitic carbon, are used as support materials [1,3,5–7]. For example, in the liquid-phase hydrogenation of cinnamaldehyde with carbon-nanotube-supported ruthenium catalysts [7–9], selectivities to cinnamyl alcohol up to 92% are observed, whereas alumina-supported ruthenium catalysts [6] give rise to selectivities of 20–30% and active carbon-supported ruthenium catalysts [10] to 30–40%. Often the increased selectivity to the unsaturated alcohol is explained in terms of a transfer of the π-electrons from the graphitic planes to the metal particles [7,8,11]. In this way the charge density on the metal increases, thus decreasing the probability for the C=C bond activation.

Although this explanation might be true, it is important to realize that at least two other factors direct the selectivity of carbon supported catalysts too, namely the metal particle size and the presence of oxygen-containing surface groups. It is well established that the cinnamyl alcohol selectivity increases with increasing particle size and that this effect is particularly pronounced with particles larger than 3 nm [3]. Coloma et al. [12,13] emphasized the importance of oxygen-

* Corresponding author.
E-mail address: k.p.dejong@chem.uu.nl (K.P. de Jong).

0021-9517/03/$ – see front matter
doi:10.1016/S0021-9517(02)00081-7

containing surface groups on carbon supports. In their study on the gas-phase hydrogenation of crotonaldehyde over platinum on activated carbon catalysts, they found an increased selectivity to the alcohol with a larger amount of oxygen-containing groups on the carbon surface. Later on, Bachiller-Baeza et al. [14] disputed the influence of the oxygen groups on the hydrogenation of crotonaldehyde over graphite-supported platinum and ruthenium catalysts. However, in both studies relatively large particles, in the range of 3–10 nm, were used and the particle sizes of the samples with different concentrations of oxygen-containing surface groups were different.

The above demonstrates that more insight into the role of the oxygen-containing surface groups in the catalytic performance of carbon-supported catalysts can only be gained if a well-defined catalyst system is available. This requires a well-defined carbon support without contaminants and micropores, metal particles smaller than 3 nm with a narrow particle size distribution, and a tunable number of surface oxygenates. Because of the importance of the features of the catalyst, we will report in detail on its preparation and characterization.

The catalyst system includes carbon nanofibers (CNF) of the fishbone type as the graphitic support material, activated by surface oxidation, and the homogeneous deposition precipitation (HDP) technique is used to apply the metal precursor phase. Small-diameter CNF (10–50 nm) can be grown from decomposition of carbon-containing gases (CH_4, CO, C_2H_2) on small metal particles of similar sizes [15,16]. They have a relatively large and accessible external surface area (100–200 m^2/g) and a well-defined graphitic structure, do not contain impurities, and are mechanically strong and chemically inert [15,16]. The fibers themselves contain no pores, but because they interweave during growth, larger mesoporous skeins are obtained. The hydrophobic and inert nature of the graphitic CNF brings along a problem: the application and anchoring of the catalytically active phase. However, the surface can be modified by treatment of the CNF in concentrated nitric acid. In this way oxygen-containing surface groups are introduced, enabling the anchoring of the active phase or its precursor and obtaining the wettable surface necessary for the aqueous solution of the metal precursor [17–20]. Moreover, concurrently, exposed nickel is extracted. The number of oxygen-containing groups on the CNF surface can be tuned by treatment in inert atmosphere at various temperatures, which (partly) removes the surface groups.

Several investigators have already demonstrated the great potential of CNF and related materials as support material. Metals such as Pt [21,22], Pd [15,23–25], Pt/Ru [26,27], Ru [8,28–30], Fe [31,32], Co [33], and Ni [34–38] have been applied on CNF and tested in various reactions, such as selective hydrogenations. In the literature diverse methods have been presented to apply the active phase, mostly incipient wetness impregnation (e.g., [23,30,33,37]), but also adsorption (e.g., [8]), ion exchange (e.g., [15]), and electroless plating (e.g., [38]). Unfortunately it appears that these procedures do not result in both a relatively high dispersion and a narrow particle-size distribution. With ion exchange, for example, Hoogenraad et al. [15,25] applied palladium on CNF and found a maximum metal loading of 3 wt%. Using adsorption Planeix et al. [8] applied 0.2 wt% Ru on carbon nanotubes, resulting in relatively large ruthenium particles, in the range of 3–7 nm. Also, when nickel, with a loading of 5 wt%, is deposited on CNF through incipient wetness impregnation, substantially larger particles are found, in the range of 2–22 nm, with an average of 8.1 nm [36]. We therefore explored the HDP technique as developed by Geus et al. and Che et al., which is very successful in the production of highly loaded and well-dispersed catalysts on oxidic support materials [40–43].

In this paper we will demonstrate that the CNF-supported ruthenium catalysts thus prepared fulfill the formulated requirements of a well-defined catalyst system, which enables systematic study of the influence of oxygen-containing surface groups on activity and selectivity in the liquid-phase hydrogenation of cinnamaldehyde.

2. Experimental

2.1. Carbon nanofiber growth

For the growth of CNF 20 wt% Ni/SiO_2 was prepared by homogeneous deposition precipitation (HDP) as described by van Dillen et al. [40] using silica (Degussa, Aerosil 200), nickel nitrate (Acros), and urea (Acros). After filtering the catalyst precursor was dried at 393 K and calcined in static air at 873 K (heating rate 5 K/min) for 2 h.

One gram of the Ni-catalyst precursor was placed in a quartz reactor. Prior to the fiber growth the Ni-catalyst was reduced in situ for 2 h in a flowing stream of a mixture of H_2 (80 ml/min) and N_2 (320 ml/min) at 1 bar and 973 K (heating rate 5 K/min). Next, the CNFs were grown at 823 K in a mixture of CO (80 ml/min), H_2 (28 ml/min), and Ar (292 ml/min) for 24 h.

The CNFs were refluxed for 1 h in a 1 M KOH solution in order to remove the silica support. For the activation of the CNFs and the removal of nickel, the CNFs were refluxed in concentrated nitric acid for 2 h and washed thoroughly with demiwater.

2.2. Synthesis of carbon nanofiber-supported ruthenium catalyst

Ruthenium (5 wt%) was deposited on the fibers according to the HDP method as follows. To an acidified suspension (pH 0.5) of 5 g CNF in 250 ml demiwater heated up to 363 K, 1.56 g of urea (Acros) and 0.82 grams (5 wt%) of $RuNO(NO_3)_3 \cdot nH_2O$ (Acros) were added under vigorous stirring. The pH of the slurry was monitored continuously.

Table 1
Sample codes and treatment conditions of the various carbon-nanofiber-supported ruthenium catalysts

Sample name	Loading (wt%)	Gas-phase prereduction	Heat treatment in N_2
RuCNFnp[a]	5.0	–	–
RuCNF	5.0	473 K	–
RuCNF573	5.0	473 K	573 K
RuCNF773	5.0	473 K	773 K
RuCNF973	5.0	473 K	973 K

[a] np = no prereduction in the gas phase.

After 6 h the loaded CNF were filtered and washed thoroughly with demiwater, dried at 393 K, and reduced with H_2 at 473 K for 1 h (heating rate 5 K/min). Following reduction the samples were exposed to air. In line with extensive experience in our lab [20], under ambient conditions further oxidation of the (graphite) CNF surface does not take place.

In order to introduce different concentrations of oxygen-containing groups onto the CNF surface, samples of the freshly reduced catalyst were heat-treated in a nitrogen atmosphere for 2 h at 573, 773, and 973 K, to remove (part of) the oxygen-containing groups. The catalyst samples, together with their identification codes, are listed in Table 1.

2.3. Catalyst and carbon nanofiber characterization

The numbers of acid sites of the oxidized CNF after the various heat-treatments were determined by performing standard acid–base titrations. For this purpose 20–40 mg of oxidized CNF was stirred with 25 ml of a solution containing 0.1 M NaCl and 0.1 mM oxalic acid in demiwater, acidified to pH = 3 with HCl. While stirring, pure nitrogen was bubbled through the slurry and 10 mM NaOH was added dropwise from a buret until the endpoint had been reached. All acid sites with $pK_a < 7.5$ were measured.

The CNF and the CNF-supported ruthenium catalysts were examined in a Philips CM-200 FEG TEM operated at 200 kV. Samples were prepared by suspending the fibers in ethanol under ultrasonic vibration. Some drops of the suspension thus produced were brought onto a holey carbon film on a copper grid.

TPR measurements were performed with a TPDRO 1100 instrument from Thermo Quest CE Instruments.

Specific surface areas (BET) were calculated from nitrogen physisorption data measured at 77 K with a Micromeretics ASAP 2400 apparatus. Prior to the physisorption experiments the samples were evacuated at 473 K for at least 16 h. Ruthenium loadings were determined using inductively coupled plasma emission spectrometry on a Vista AZ CCD simultaneous ICP-AES.

XPS analyses were performed on a Quantum 2000 Scanning SK Microprobe instrument using Al-K_α radiation. Before the analysis all samples were reduced again in hydrogen at 383 K (heating rate 4 K/min) for 30 min. Semiquantitative data were calculated from the survey scans. The narrow scan data were used to determine the oxidation state and/or compounds for the Ru and C peaks. This was accomplished from a Gauss–Lorenzian peak fit of the appropriate photoelectron peaks.

Hydrogen chemisorption measurements were performed using a Micromeritics ASAP 2010C. Before the chemisorption measurements, each sample was dried in He at 393 K for 1 h, and reduced in flowing H_2 (flow rate = 50 ml/min STP) at 473 K for 2 h (heating rate 5 K/min). After reduction the catalyst was degassed for 2 h at 10^{-1} Pa at the reduction temperature in order to eliminate chemisorbed hydrogen and water. The isotherms were measured at 308 K. The H/Ru ratios are based on the amounts adsorbed at zero pressure, found by extrapolation of the linear part of the isotherm. Calculations are made either with the total amount of adsorbed hydrogen or with the amount of strongly adsorbed hydrogen. Estimated average particle sizes and dispersions are based on spherical geometry and an adsorption stoichiometry of $H/Ru_s = 1$. The average Ru particle size, d, was calculated from

$$d * D = \frac{M * 6 * \rho_{\text{site}}}{\rho_{\text{metal}} * N},$$

where d is the ruthenium particle size, D is the dispersion, M is the molecular weight (Ru = 101 g/mol), ρ_{site} is the ruthenium surface site density (16.3 Ru atoms/nm^2), ρ_{metal} is the metal density (Ru 12.3 g/cm^3), and N is the Avogadro number (6.022×10^{23} mol^{-1}), giving $d = 1.33/\text{D}$ (nm) [44].

2.4. Catalytic experiments

Hydrogenation of cinnamaldehyde was studied in batch mode in a 200-ml autoclave equipped with a stirrer, a sample port, a reagent injection port, a gas inlet, and a vent. The sample tube was equipped with a filter at its end to prevent carry over of catalyst particles during sampling.

The prereduced and heat-treated catalysts (0.5–1 g) were reactivated in *i*-propanol (100 ml) at 383 K and 4.5 MPa H_2 pressure for 30 min in the autoclave (1250 rpm) prior to the introduction of cinnamaldehyde ($\sim$ 9 grams). All the reactions were conducted under the above conditions. Micro samples were withdrawn periodically and analyzed on a gas chromatograph (Hewlett Packard 6890 Series with autosampler) using an HP5Cpsil8 capillary column (30 m $\times$ 0.32 mm ID). The calibration was done by using synthetic mixtures of pure compounds in isopropanol. Methylbenzoate was used as an internal standard.

The experimental cinnamaldehyde concentration versus time data are approximated by a rate law that is first order with respect to the reactant. Accordingly, catalytic activities are compared on the basis of the first-order rate constant from a regression fit of the experimental data in the expression,

$$\ln\left\{\frac{[\text{CALD}]_t}{[\text{CALD}]_0}\right\} = -kt,$$

where $[CALD]_t$ = the cinnamaldehyde concentration at time t and $[CALD]_0$ = the cinnamaldehyde concentration at the beginning of the reaction.

3. Results

3.1. Characterization of the carbon nanofiber support

The CNFs were of the fishbone type, i.e., with the graphite planes oriented at an angle to the central axis. After removal of the growth catalyst and activation treatment with nitric acid the nonmicroporous fibers exhibited a surface area of 177 m^2/g. In Fig. 1 a SEM image of an untreated CNF sample is shown. Clearly the mesoporous structure of the CNF skeins is visible. The lighter spots in the image, situated on top of the fibers, are nickel particles from which the fibers had been grown. X-ray diffraction and TEM-images demonstrated that the graphitic structure had not been affected during activation. From SEM and TEM micrographs an average fiber diameter of 25 nm with a narrow diameter distribution could be derived.

As stated earlier, the activation procedure in nitric acid is carried out to introduce various types of oxygen functional groups on the CNF and to remove nonencapsulated nickel from the growth catalyst. The remaining nickel ($\leqslant 0.5$ wt%, XRF analysis) is shown from TEM to be encapsulated by graphitic envelopes thus preventing interference in catalysis.

Table 2 lists the number of acid sites ($pK_a < 7.5$) of oxidized CNF treated at different temperatures, as determined by titration. Activation of the CNF resulted, after drying at 393 K, in 1.28 acid sites/nm^2 and heat treatment indeed in removal of part of the oxygen-containing groups: after treatment at 573 K 0.96 acid sites/nm^2 were present and after treatment at 773 K and 973 K only 0.20, respectively 0.03, acid sites/nm^2 remained.

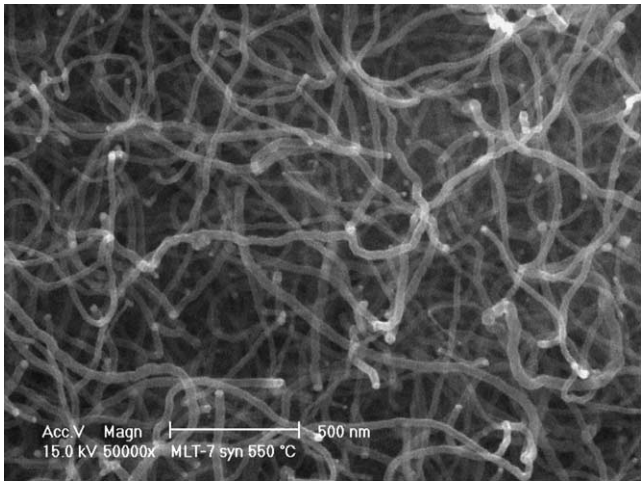

Fig. 1. SEM image of untreated carbon nanofibers.

Table 2
Number of acid sites on CNF surface as a function of heat treatment temperature determined with acid-base titration

Sample name	Number of acid site/nm^2
Oxidized CNF	0.62
Oxidized CNF—573 K in N_2	0.48
Oxidized CNF—773 K in N_2	0.10
Oxidized CNF—973 K in N_2	0.02

3.2. Characterization of the carbon-nanofiber-supported ruthenium catalysts

The metal loading of the Ru/CNF catalysts as established with ICP corresponded to the intended ruthenium loading of 5 wt%. TPR results (not shown) of the fresh catalyst demonstrated that the catalysts were completely reduced at 473 K. Therefore all catalysts were reduced at this temperature. RuCNFnp was only reduced in situ at 383 K in the liquid phase before the catalytic experiments to maintain a larger fraction of the oxygen-containing surface group on the catalyst. With XPS we checked the oxidation state of the reduced and heat-treated catalysts. In Table 3 the ruthenium $3p_{3/2}$ and $3d_{5/2}$ binding energies determined using Gauss–Lorenzian peak fits are displayed. The results showed that RuCNF, RuCNF573, RuCNF773, and RuCNF973 all show the same binding energy, indicating similar oxidation states for all samples. Only RuCNFnp is slightly shifted to higher binding energies. RuCNFnp is probably less reduced because some ionic Ru species still might be present because of the mild reduction treatment.

In Figs. 2A and 2B two representative TEM images of reduced RuCNF are shown. The ruthenium particles appear as dark dots on the surface of the CNF. The images show homogeneous coverage with small ruthenium particles. In Fig. 2B the fishbone orientation of the graphitic planes is also visible. The ruthenium particle size distribution is very narrow. A range of 1.1–2.2 nm has been established with an average particle size of 1.5 nm. Using the HDP method we have prepared several CNF-supported ruthenium catalysts and the results convincingly demonstrate the reproducibility of the preparation method.

After heat treatment in inert atmosphere the catalysts are also characterized with TEM. In Figs. 3A and 3B TEM

Table 3
Ruthenium $3p_{3/2}$ and $3d_{5/2}$ binding energies of the carbon nanofiber-supported ruthenium catalysts determined by XPS using Gauss–Lorenzian peak fits

Sample name	Treatment in XPS	E_{bin} (eV)	
		Ru $3p_{3/2}$	Ru $3d_{5/2}$
RuCNFnp	None	465	283.8
RuCNFnp	Red 383 K	463.2	281.1
RuCNF	Red 383 K	462.4	280.8
RuCNF573	Red 383 K	462.1	280.9
RuCNF773	Red 383 K	462.3	280.9
RuCNF973	Red 383 K	462.8	281.1

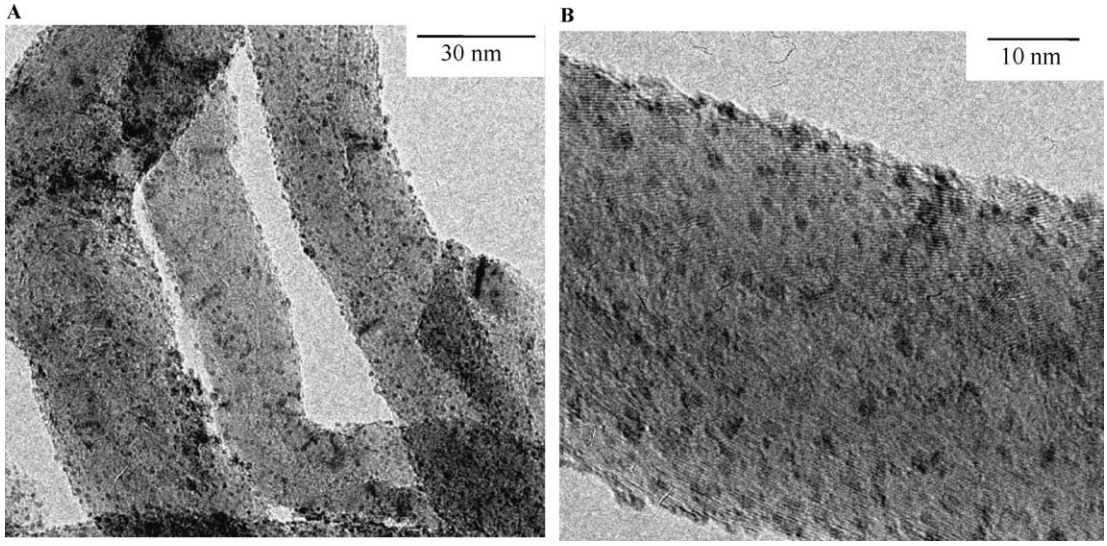

Fig. 2. TEM images of 5 wt% carbon-nanofiber-supported ruthenium catalysts after reduction.

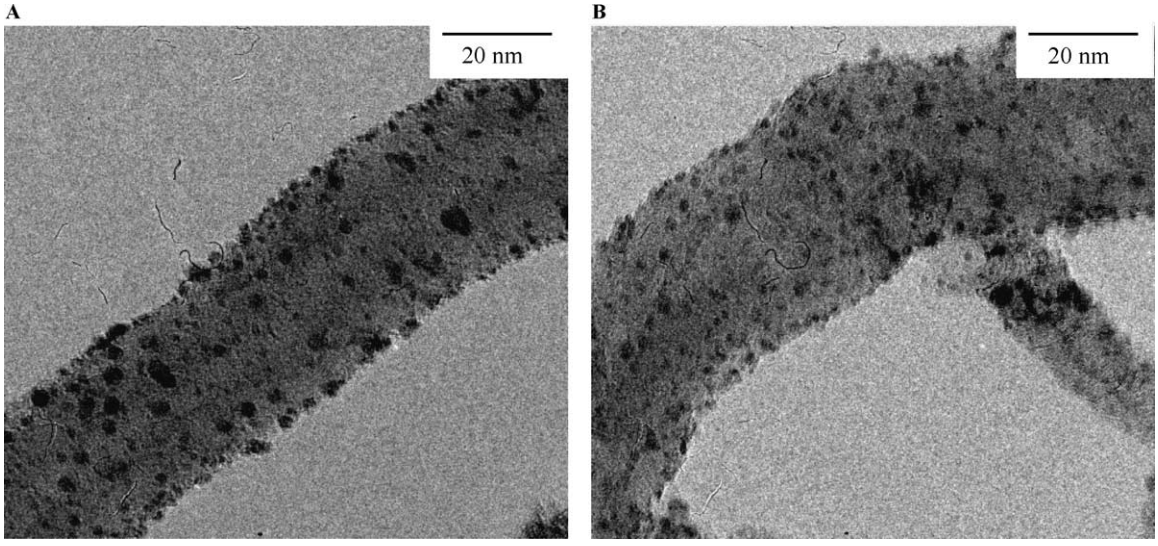

Fig. 3. TEM images of 5 wt% carbon-nanofiber-supported ruthenium catalysts after reduction and heat treatment in N_2 at (A) 773 and (B) 973 K.

images of RuCNF773 and RuCNF973 are displayed. The ruthenium particles are slightly larger after heat treatment, but many very small particles are still present too. Some sintering causes broadening of the particle size distribution and a small increase in the average particle size. The average particle sizes calculated from the TEM images are presented in Table 4, along with the average particle sizes calculated from the hydrogen chemisorption data. These last values are in close agreement with the estimated TEM values if the total amount of adsorbed hydrogen is used for the calculations. Also, hydrogen chemisorption shows a small decrease in H/Ru ratio for the catalysts heat-treated under inert atmosphere.

3.3. Hydrogenation of cinnamaldehyde

The hydrogenation of cinnamaldehyde can be presented by a simplified reaction pathway, as shown in Fig. 4. Additionally, various side-reactions can occur. For instance, in this study in some cases 3-propoxy-1-propenyl-benzene is formed (Table 6). This product forms via the reaction between β-methylstyrene, a hydrogenolysis product of cinnamyl alcohol, and the solvent isopropanol.

Table 4
TEM and hydrogen chemisorption results on the different carbon nanofiber-supported ruthenium catalysts

Sample	TEM	H_2-Chemisorption			
	d (nm)	Irreversible		Total	
		H/Ru	d (nm)	H/Ru	d (nm)
RuCNF	1.5 ± 0.2	0.40	3.4	0.74	1.8
RuCNF573	nd[a]	0.45	3.0	0.70	1.9
RuCNF773	2.2 ± 0.6	0.38	3.5	0.64	2.1
RuCNF973	1.8 ± 0.7	0.25	5.3	0.44	3.0

[a] nd = not determined.

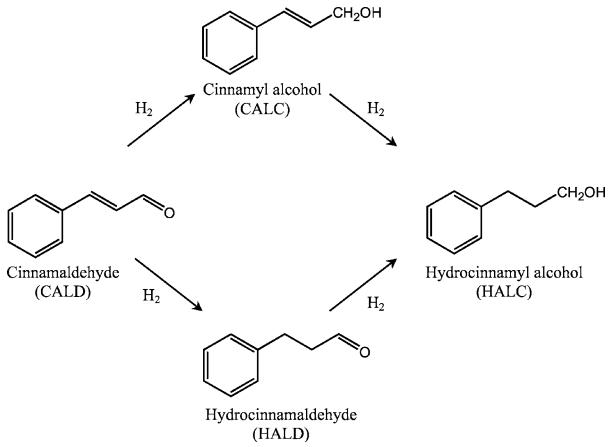

Fig. 4. Reaction pathway of the hydrogenation of cinnamaldehyde.

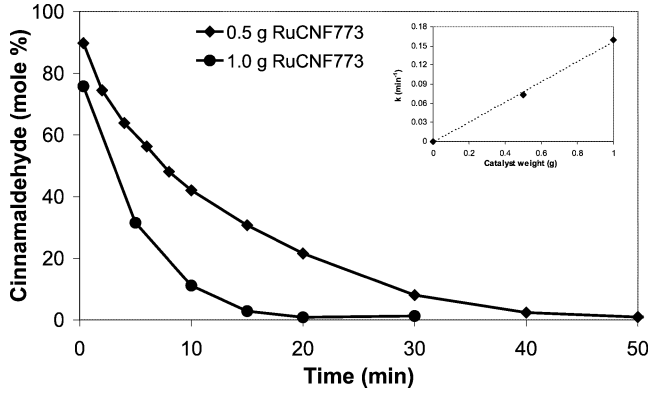

Fig. 5. Catalytic activity of RuCNF773 for cinnnamaldehyde hydrogenation; effect of the catalyst amount.

The reproducibility of the catalytic experiments and the absence of gas–liquid diffusion limitations were checked by varying the amount of catalyst used for the catalytic measurements. In Fig. 5 the decrease in reactant concentration (mol%) is displayed versus time for 0.5 and 1 g of RuCNF773 and in the small inserted graph the first-order rate constants are plotted versus catalyst weight. A linear relation is observed between the amount of catalyst and the volume-based rate constant, demonstrating the reliability of the catalytic tests.

Figure 6 shows product distributions obtained with RuCNF and RuCNF973. For reasons of clarity only the amounts of cinnamaldehyde (CALD) and the primary reaction products hydrocinnamaldehyde (HALD) and cinnamyl alcohol (CALC) are plotted. An exponential decrease in the cinnamaldehyde concentration is observed as a function of time with a concurrent increase in the concentrations of the reaction products. This shows that the reaction is first order with respect to cinnamaldehyde. In Table 5 the calculated rate constants, the relative rate constants compared to the measured rate with RuCNFnp, and the TOF values are given. From Fig. 6 and Table 5 the large difference in catalytic performance as a function of treatment temperature is distinct. A significant increase in total activity is observed with increasing treatment temperature of the CNF-supported ruthenium catalysts. The activity is enhanced by a factor of 22 when the treatment temperature is increased from 383 K, the reduction temperature of RuCNFnp, to 973 K (RuCNF973). The same trend is noticed with the TOF values. This increase in activity can be mainly ascribed to a large increase in aldehyde (HALD) formation, as can be seen in Fig. 7. The activity for cinnamyl alcohol formation increases only slightly as a function of the catalyst treatment temperature. Apparently, hydrogenation of the C=C bond is enhanced when less oxygen-containing groups are present on the surface.

The selectivities for the different reaction products at 60% conversion are represented in Table 6. From this table it is clear that not only the activity but also the selectivity highly depends on the pretreatment temperature of the Ru/CNF catalysts. RuCNFnp gives an S_{HALD} of 34% and an S_{CALC} of 48%. At higher treatment temperatures S_{CALC} drops and S_{HALD} increases. RuCNF973 is very selective to hydrocinnamaldehyde with $S_{HALD} > 70\%$. This large change in selectivity is mainly caused by the increased activity for C=C hydrogenation.

4. Discussion

The aim of our study was to reveal the effect of oxygen-containing surface groups of CNF-supported ruthenium catalysts on catalytic performance in the selective hydrogena-

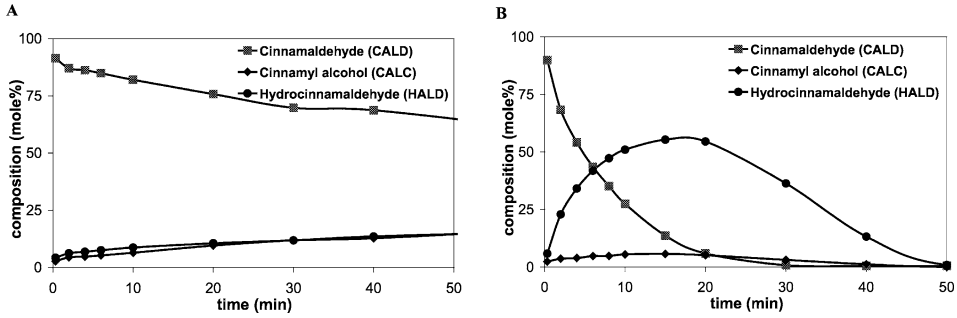

Fig. 6. Cinnamaldehyde conversion and product distribution as a function of time on stream obtained at 383 K and 4.5 MPa hydrogen over carbon-nanofiber-supported ruthenium catalysts (A) RuCNFnp and (B) RuCNF973.

Table 5
Activity for cinnamaldehyde hydrogenation with carbon-nanofiber-supported ruthenium catalysts, calculated from the time needed to obtain 60% conversion

Sample name	Rate constant (min^{-1})	Rel. rate constant[b]	TOF (s^{-1})[a]
RuCNFnp	6.2×10^{-3}	1.0	nd[c]
RuCNF	8.2×10^{-3}	1.3	0.03
RuCNF573	1.7×10^{-2}	2.7	0.08
RuCNF773	7.4×10^{-2}	12	0.31
RuCNF973	1.4×10^{-1}	22	0.83

[a] Results are given in mole CALD hydrogenated per mole of ruthenium surface atoms in the catalyst per second. The number of ruthenium surface atoms is calculated from the catalyst weight, the metal loading, and the H/Ru (total H) ratio.

[b] The relative rate constant is the rate constant divided by the rate constant of RuCNFnp.

[c] nd not determined because the H/Ru ratio is not known for this sample.

Table 6
Selectivity to cinnamyl alcohol, hydrocinnamaldehyde, hydrocinnamyl alcohol and a byproduct for cinnamaldehyde hydrogenation with carbon-nanofiber-supported ruthenium catalysts. Determined at 60% conversion

Sample name	Byproduct			
	S_{CALC} (%)	S_{HALD} (%)	S_{HALC} (%)	(3-propoxy-1-propenyl benzene)
RuCNFnp	48	34	18	–
RuCNF	43	33	16	8
RuCNF573	30	33	14	23
RuCNF773	13	48	13	26
RuCNF973	8	73	12	7

tion of cinnamaldehyde. From the literature it is known that, to be able to discriminate the effect of the surface groups from the effect of the particle size of the active metal, it is necessarry to use a catalyst with a narrow and constant size distribution and a high dispersion with, preferably, a mean particle size < 3 nm [3]. The results presented demonstrate that we, using the HDP procedure, succeeded in the design of such a catalyst with a mean size in the range of 1–2 nm.

Using ion exchange the number of acidic groups of the freshly activated fibers could have given rise, taking 1.28 groups/nm^2, to a ruthenium loading of at most 2–3 wt%, which is close to the experimental results of Hoogenraad et al. [15,25]. For this calculation we assumed one ruthenium precursor molecule per acidic site. These authors used ion-exchange to apply palladium on CNF and found a metal loading of around 3 wt% at most. This implies that an alternative method had to be used to obtain a 5 wt% CNF supported ruthenium catalyst.

The CNF used for this study are entirely graphitic and very uniform, as shown in the SEM images in Fig. 1. By treatment in boiling nitric acid, oxygen-containing surface groups were introduced, while the graphitic character of the CNF was maintained. It turned out that the number of oxygen-containing surface groups could be tuned by

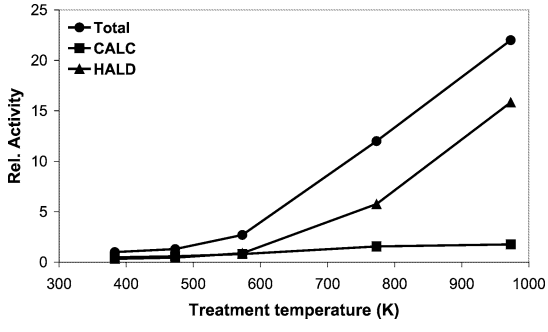

Fig. 7. Relative activity for CALD hydrogenation (●), for production of CALC (■), and for production of HALD (▲) after different pretreatment temperatures of Ru/CNF.

treatment in nitrogen at different temperatures, as was established with titration experiments (Table 2).

We applied the HDP technique to deposit ruthenium on the oxidized CNF. TEM images (Figs. 2 and 3) and chemisorption data (Table 4) demonstrate that with this technique reproducibly highly dispersed catalysts with narrow particle size distributions could be prepared. In the procedure the precipitating agent, in this case hydroxyl ions, is introduced slowly and homogeneously via urea hydrolysis at 363 K. Production and consumption of hydroxyl ions is balanced in such a way that nucleation of the ruthenium precursor in the liquid phase is avoided and exclusively is anchored to the support. Under these conditions oxidic support materials form a surface compound [40–43]. On carbon supports no surface compounds are formed [39] and probably the interaction is confined to that of the precursor ions with a relatively low number of surface sites. However, the results clearly show the applicability of the HDP technique to the preparation of CNF-supported metal catalyst.

When the average particle sizes calculated from TEM images and derived from H_2-chemisorption are compared (Table 4) it appears that the particle sizes based on the total amount of adsorbed hydrogen correspond best to the TEM results. In the literature often only the strongly adsorbed hydrogen is taken to calculate the dispersion, but XAFS results of Oudenhuijzen et al. with Pt/Al_2O_3 catalysts unambigiously show the presence of a Pt–H antibonding state for both weakly and strongly bonded hydrogen [45]. This demonstrates that with this type of metals weakly bonded hydrogen is also chemisorbed to the metal particles and should be taken into account in the determination of the dispersion and the mean particle size.

Upon heating under inert atmosphere some sintering occurs (Table 4). The average particle sizes become slightly larger after heating at 973 K and the particle size distributions somewhat broader. Nevertheless the sintering is very limited, taking into account the treatment temperatures up to 973 K. This demonstrates the very high thermostability of the catalysts and the surprisingly strong bond between the CNF support and the ruthenium metal particles. The exact nature of the metal–support interaction is not clear yet.

In the literature it is well established that when oxygen-containing groups on a carbon support are heated under inert atmosphere, carboxyl groups are already decomposed at temperatures beyond 473 K [19,20]. However, the largest influence on the catalytic performance is expected from oxygen groups other than carboxylic groups that are still present and are in direct contact with the ruthenium particles. The titration results presented in Table 2 also show that simply by heating at different temperatures CNF can be obtained with a varying and well-defined number of acidic oxygen-containing surface groups, enabling our study on the effect of these groups on catalysis. It is important to note that upon the activation of CNF, besides oxygen-containing groups on the surface, ether-type oxygen groups are also formed in between the graphitic layers [20]. The thermostability of these groups is rather high: decomposition under inert atmosphere starts at circa 873 K. These groups are not probed with titration, but they can also have an influence on the catalytic system.

In the hydrogenation of cinnamaldehyde large differences are found between the differently pretreated catalysts in the activity and the selectivity. The total activity strongly increases with increasing treatment temperature of the Ru/CNF catalysts (Table 5). This large increase in activity is mainly caused by a rise in the activity for the hydrogenation of the C=C bond, yielding hydrocinnamaldehyde, while the activity for the hydrogenation of the carbonyl bond increases only slightly (Fig. 7). Consequently, the selectivity for cinnamyl alcohol drops and the hydrocinnamaldehyde selectivity rises with increasing pretreatment temperature.

From TPR and XPS results it appears that RuCNF, RuCNF573, RuCNF773, and RuCNF973 are completely reduced. Very small numbers of ionic ruthenium species can still be present in these samples, but their occurrence is not obvious from the XPS data. RuCNFnp can still contain larger amounts of ionic ruthenium; however, the largest changes in activity and selectivity are found for the samples treated at higher temperature, meaning that a variance in oxidation state most likely does not bring about the observed effects.

Also, a particle size effect cannot account for the observed changes in selectivity. The ruthenium particle sizes of the catalysts hardly differ, notably not with RuCNFnp, RuCNF, RuCNF573, and RuCNF773, and all catalysts have particles < 3 nm (Table 6). Besides, it is well established that the cinnamyl alcohol selectivity increases with increasing ruthenium particle size and this effect is particularly pronounced with ruthenium particles larger than 3 nm [3]. Here, the trend is opposite. We therefore conclude that, because the particle size effect has to be excluded, the change in catalytic performance is related to the difference in the concentration of oxygen-containing surface groups.

The best illustration to this is given in Fig. 8, in which the relative total activity for cinnamaldehyde hydrogenation is plotted versus the amount of acidic surface groups/nm^2 present on the CNF surface. Because determination of the oxygen-containing groups of the Ru/CNF catalysts themselves could not be effectuated because of disturbance of the titration experiments by the ruthenium phase, we have taken in this figure as second-best choice the values found with the freshly activated CNF support. A nice correlation is observed between the activity and the acidity of the support. When only few acidic groups are present the activity is high and with increasing surface acidity the activity drops. This correlation is not a direct cause-and-effect relation. Besides the acidic groups other oxygen-containing surface groups are also present on the CNF surface. But the measured shift in activity gives a strong indication that the amount of oxygen incorporated into the CNF plays an important role in the catalytic performance.

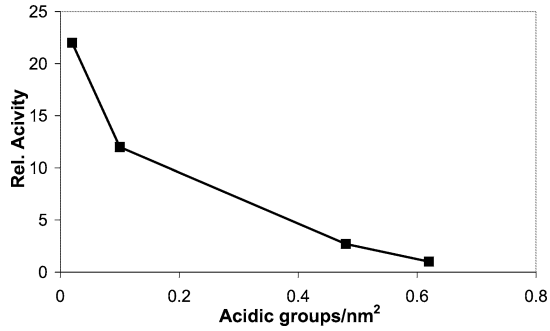

Fig. 8. Relative total activity for cinnamaldehyde hydrogenation as a function of the number of acidic groups/nm^2 on the bare carbon nanofiber surface.

The most current explanation for the effect of the oxygen-containing surface groups on the catalytic performance is the effect of the polarity of the CNF support. At increasing treatment temperatures, the CNF surface changes gradually from polar to nonpolar due to the removal of the oxygen-containing surface groups. This change in polarity can change the preferential adsorption mode of cinnamaldehyde and, thus, a shift in selectivity. English et al. [46] found an enhanced selectivity to crotonalcohol for Pt/TiO_2 after high-temperature reduction due to an increased polarity at the metal surface. This increased polarity was caused by a decoration of the surface of the Pt crystallites with titania suboxides (TiO_x) that act as relatively by strong electron-pair acceptor sites for the free electron pairs at the oxygen of the carbonyl group. Thus, the increased polarity leads to an activation of the C=O bond of crotonaldehyde and enhances the rate of C=O bond hydrogenation. This model cannot fully explain our results with respect to the hydrogenation of cinnamaldehyde. Although it accounts for the shifts in selectivity, it does not clarify the significant increase in the hydrogenation rate of C=C bond and the slight increase in C=O bond hydrogenation with decreasing polarity.

An alternative explanation implies the influence of the oxygen-containing groups present on the CNF surface on the electronic state of ruthenium. This model is based on the work of Koningsberger and co-workers and concerns metal–oxidic support interaction [47–49]. These authors state that, due to the effect of the support, the Fermi level

of the metal particles shifts to a higher binding energy with decreasing electron richness of the support oxygen atoms. For the current CNF-supported ruthenium catalysts this model suggests that lower amounts of (electronegative) oxygen in the carbon support give rise to lowering of the ruthenium Fermi level. A lowering of the Fermi level may invoke stronger adsorption of the C=C bond, thereby enhancing its rate of hydrogenation.

At the moment we cannot conclude which explanation holds or if a combination of the two effects causes the changes in activity and selectivity. Further studies using XPS, EXAFS, and XANES are in progress to further clarify the influence of the oxygen-containing groups on the hydrogenation of cinnamaldehyde over metal CNF catalysts.

5. Conclusions

Using homogeneous deposition precipitation, carbon-nanofiber-supported ruthenium catalysts were prepared with a narrow and constant size distribution, a high dispersion, and a mean particle size < 3 nm. By treatment of carbon nanofibers in nitric acid and, subsequently, heat treatment in nitrogen atmosphere, the number of oxygen-containing groups on the carbon nanofiber surface was tuned.

A clear trend was observed in activity and selectivity in the liquid phase hydrogenation of cinnamaldehyde with decreasing numbers of oxygen-containing surface groups. The rate of cinnamaldehyde conversion was enhanced by a factor of 22 after removal of the acid oxygen groups. This enhanced activity is mainly caused by a strong increase in the hydrogenation rate of the C=C bond, while only a slightly increased C=O bond hydrogenation occurs. Due to this, a large shift in selectivity towards hydrocinnamaldehyde was observed. This unambiguously demonstrates the important influence of the surface-oxygen functionalities on the catalytic performance. The exact mechanism of this influence is currently under investigation.

Acknowledgments

The authors are grateful to C. van der Spek for performing the TEM measurements and to DSM Research for the catalysis experiments. Prof. Dr. M.R. Egmond and R. Dijkman of the Department Membrane Enzymology and Drs. J.M.P. van Heeswijk are acknowledged for the titration experiments. These investigations are supported by Sasol Technology R&D and the Council for Chemical Sciences of the Netherlands Organization for Scientific Research with financial aid from the Netherlands Technology Foundation (CW/STW 349-5357).

References

[1] P. Kluson, L. Gerveny, Appl. Catal. A 128 (1995) 13.
[2] V. Ponec, Appl. Catal. A 149 (1997) 27.
[3] B. Coq, F. Figueras, Coord. Chem. Rev. 178–180 (1998) 1753.
[4] P. Gallezot, D. Richard, Catal. Rev.-Sci. Eng. 40 (1998) 81.
[5] A. Giroir-Fendler, D. Richard, P. Gallezot, Stud. Surf. Sci. Catal. 41 (1988) 171.
[6] B. Coq, P.S. Kumbhar, C. Moreau, P. Moreau, M.G. Warawdekar, J. Mol. Catal. 85 (1993) 215.
[7] P.S. Kumbhar, B. Coq, C. Moreau, P. Moreau, J.M. Planeix, M.G. Warawdekar, in: N.M. Gupta, D.K. Chakrabarty (Eds.), Catalysis: Modern Trends, Narosa Publishing House, New Delhi, 1995.
[8] J.M. Planeix, N. Coustel, B. Coq, V. Brotons, P.S. Kumbhar, R. Dutartre, P. Geneste, P. Bernier, P.M. Ajayan, J. Am. Chem. Soc. 116 (1994) 7935.
[9] M. Lashdaf, A. Hase, E. Kauppinen, A.O.I. Krause, Catal. Lett. 52 (1998) 199.
[10] S. Galvagno, G. Capanelli, G. Neri, A. Donato, R. Pietropaolo, J. Mol. Catal. 64 (1991) 237.
[11] T. Vergunst, F. Kapteijn, J.A. Moulijn, Catal. Today 66 (2001) 381.
[12] F. Coloma, A. Sepúlveda-Escribano, F. Rodríguez-Reinoso, Appl. Catal. A 123 (1995) L1.
[13] F. Coloma, A. Sepúlveda-Escribano, J.L.G. Fierro, F. Rodríguez-Reinoso, Appl. Catal. A 150 (1997) 165.
[14] B. Bachiller-Baeza, A. Guerrero-Ruiz, I. Rodríguez-Ramos, Appl. Catal. A 192 (2000) 289.
[15] M.S. Hoogenraad, PhD thesis, Utrecht University, 1995.
[16] K.P. de Jong, J.W. Geus, Catal. Rev.-Sci. Eng. 42 (2000) 482.
[17] F. Rodriguez-Reinoso, Carbon 36 (1998) 159.
[18] R.J.J. Jansen, PhD thesis, Delft University, 1994.
[19] H.P. Boehm, Adv. Catal. 16 (1966) 179.
[20] T.G. Ros, A.J. van Dillen, J.W. Geus, D.C. Koningsberger, Chem. Eur. J. 8 (2002) 1151.
[21] R.T.K. Baker, K. Laubernds, A. Wootsch, Z. Paál, J. Catal. 193 (2000) 165.
[22] C.A. Bessel, K. Laubernds, N.M. Rodriguez, R.T.K. Baker, J. Phys. Chem. B 105 (2001) 1115.
[23] C. Pham-Huu, N. Keller, L.J. Charbonniere, R. Ziessel, M.J. Ledoux, Chem. Commun. 1871 (2000).
[24] C. Pham-Huu, N. Keller, G. Ehret, L.J. Charbonniere, R. Ziessel, M.J. Ledoux, J. Mol. Catal. A 170 (2001) 155.
[25] M.S. Hoogenraad, R.A.G.M.M. van Leeuwarden, G.J.B. van Breda Vriesman, A. Broersma, A.J. van Dillen, J.W. Geus, Stud. Surf. Sci. Catal. 91 (1995) 263.
[26] E.S. Steigerwalt, G.A. Deluga, D.E. Cliffel, C.M. Lukehart, J. Phys. Chem. B 105 (2001) 8097.
[27] S. Hermans, J. Sloan, D.S. Shephard, B.F.G. Johnson, M.L.H. Green, Chem. Commun. 276 (2002).
[28] B. Coq, J.M. Planeix, V. Brotons, Appl. Catal. A 173 (1998) 175.
[29] T. Braun, M. Wohlers, T. Belz, G. Nowitzke, G. Wortmann, Y. Uchida, N. Pfänder, R. Schlögl, Catal. Lett. 43 (1997) 167.
[30] M. Lashdaf, A. Hase, E. Kauppinen, A.O.I. Krause, Catal. Lett. 52 (1998) 199.
[31] N.M. Rodriguez, M.-S. Kim, R.T.K. Baker, J. Phys. Chem. 98 (1994) 13108.
[32] E. van Steen, F.F. Prinsloo, Catal. Today 71 (2002) 327.
[33] Z.-J. Liu, Z.-Y. Yuan, W. Zhou, L.-M. Peng, Z. Xu, Phys. Chem. Chem. Phys. 3 (2001) 2518.
[34] S.K. Shaikhutdinov, L.B. Avdeeva, B.N. Novgorodov, V.I. Zaikovskii, D.I. Kochubey, Catal. Lett. 47 (1997) 35.
[35] F. Salman, C. Park, R.T.K. Baker, Catal. Today 53 (1999) 385.
[36] A. Chambers, T. Nemes, N.M. Rodriguez, R.T.K. Baker, J. Phys. Chem. B 102 (1998) 2251.
[37] C. Park, R.T.K. Baker, J. Phys. Chem. B 102 (1998) 5168.
[38] L.M. Ang, T.S.A. Hor, G.Q. Xu, C.H. Tung, S.P. Zhao, J.L.S. Wang, Carbon 38 (2000) 363.
[39] B.L. Mojet, M.S. Hoogeraad, A.J. van Dillen, J.W. Geus, D.C. Koningsberger, J. Chem. Soc. Faraday Trans. 93 (1997) 4371.
[40] A.J. van Dillen, J.W. Geus, L.A.M. Hermans, J. van der Meijden, Stud. Surf. Sci. Catal. 2 (1977) 677.

[41] L.A.M. Hermans, J.W. Geus, Stud. Surf. Sci. Catal. 3 (1979) 113.
[42] P. Burattin, M. Che, C. Louis, J. Phys. Chem. B 101 (1997) 7060.
[43] P. Burattin, M. Che, C. Louis, J. Phys. Chem. B 102 (1998) 2722.
[44] J.J.F. Scholten, A.P. Pijpers, A.M.L. Hustings, Catal. Rev. Sci. Eng. 27 (1985) 151.
[45] M.K. Oudenhuijzen, J.H. Bitter, D.C. Koningsberger, J. Phys. Chem. B 105 (2001) 4616.
[46] M. English, A. Jentys, J.A. Lercher, J. Catal. 166 (1997) 25.
[47] D.E. Ramaker, J. de Graaf, J.A.R. van Veen, D.C. Koningsberger, J. Catal. 203 (2001) 7.
[48] D.C. Koningsberger, J. de Graaf, B.L. Mojet, D.E. Ramaker, J.T. Miller, Appl. Catal. A 191 (2000) 205.
[49] B.L. Mojet, J.T. Miller, D.E. Ramaker, D.C. Koningsberger, J. Catal. 186 (1999) 373.